

Maximum Entropy Analysis of the 2D Density Turbulence Measured by MIR in TPE-RX

Zhongbing SHI, Yoshio NAGAYAMA¹⁾, Soichiro YAMAGUCHI²⁾, Daisuke KUWAHARA³⁾, Tomokazu YOSHINAGA¹⁾, Shoji SUGITO¹⁾, Yoichi HIRANO⁴⁾, Haruhisa KOGUCHI⁴⁾, Satoru KIYAMA⁴⁾, Hajime SAKAKITA⁴⁾, Kiyoyuki YAMBE⁴⁾, and Clive MICHAEL⁵⁾

The Graduate University for Advanced Studies, Toki 509-5292, Japan

¹⁾*National Institute for Fusion Science, Toki 509-5292, Japan*

²⁾*Kansai University, Suita 564-8680, Japan*

³⁾*Department of Energy Science, Tokyo Institute of Technology, Tokyo 152-8550, Japan*

⁴⁾*Advanced Industrial Science and Technology, Tsukuba 305-8568, Japan*

⁵⁾*UKAEA, Abingdon, Oxfordshire OX14 3DB, United Kingdom*

(Received 9 January 2009 / Accepted 22 May 2009)

Two-dimensional (2D) turbulence measurement by using microwave imaging reflectometry (MIR) has been performed in the reversed field pinch (RFP) plasma in TPE-RX. In this work, the maximum entropy method (MEM) is used to estimate the 2D k -spectrum. The turbulences between the pulsed poloidal current drive (PPCD) and the high θ plasmas are studied. The $m = 1$ modes are dominant in PPCD plasma, while in high θ plasma the k spectrum expands to the high k range and the turbulence propagates in the electron drift direction. The preliminary result shows that PPCD plasma switches off the turbulence, and the high θ plasma has strong turbulence.

© 2010 The Japan Society of Plasma Science and Nuclear Fusion Research

Keywords: turbulence, microwave imaging reflectometry, maximum entropy method

DOI: 10.1585/pfr.5.S1019

1. Introduction

Microwave reflectometry, based on the radar technique, is a powerful tool to measure the plasma density profile and density fluctuation [1, 2]. In a reflectometry system, the launching wave is reflected by the cutoff layer in the plasma. The phase difference between the launching wave and the reflection wave can be detected, and the phase fluctuation is mainly modified by the density fluctuations near the cutoff region in the one-dimensional (1D) geometric approximation [1].

However, two-dimensional (2D) configuration of the fluctuation may cause a complicated interference pattern on the detection plane due to the diffraction effects [1–4]. Microwave imaging reflectometry (MIR) uses large aperture optical technique to correct the disturbed wave front. The image of the cutoff surface is made by the wide aperture lens onto the 2D detector array located at the detector plane. The feasibilities of MIR for 2D turbulence measurement have been investigated in theories and experiments intensively [1–7].

To obtain the fine structures of the fluctuations, a big detector array is needed. However, the detector size is often smaller than the correlation length of the fluctuation. The measurement area in plasma is limited by the small window. On the other hand, the turbulent signals are often mixed with long distance correlation and short

distance correlation modes, leading to the complicated 2D cross-correlation function. The traditional two-point cross-correlation can't distinguish the multiple modes. To obtain the useful information from the limited experimental data, it is necessary to develop a new numerical method to estimate the turbulence structures from the signals obtained by a few detectors.

In this paper, we have developed a MIR system to investigate the 2D turbulence in the reversed field pinch (RFP) [8] plasma in TPE-RX. The maximum entropy method (MEM) [9, 10] is used to improve the spectral resolution. The turbulences between the pulsed poloidal current drive (PPCD) and the high θ plasmas are studied. The preliminary result shows that the PPCD plasma switches off the turbulence which agrees with the nonlinear MHD dynamo model [8]. The paper is organized as follows: Section 2 presents the MIR system in TPE-RX. The analysis methods are described in section 3. The turbulences between PPCD and the high θ plasmas are discussed in section 4. The summary is given in section 5.

2. MIR System in TPE-RX

TPE-RX is a large RFP device with major radius $R = 1.72$ m and minor radius $a = 0.45$ m [11]. The experiments with MIR have been performed with the plasma current of 200 ~ 300 kA and electron density of $(0.5-1) \times 10^{19}$ cm⁻³. Since the flat or hollow density profiles are often observed

author's e-mail: shizb@swip.ac.cn

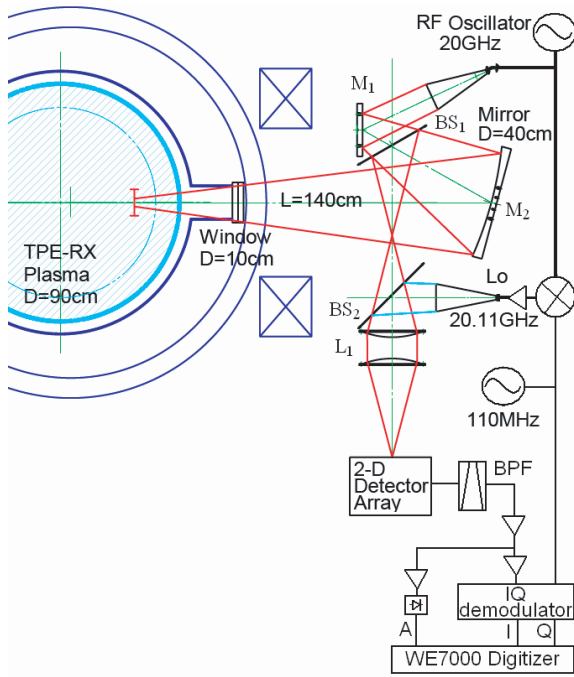


Fig. 1 Schematic diagram of the MIR system on TPE-RX

in PPCD and gas-puffing plasmas, the cutoff radius of 20 GHz is mainly located at $r_{\text{cut}}/a = 0.6 \sim 0.9$. This region is near the reversed field surface. It is useful for the calibration of the optical aberration of MIR system.

Figure 1 shows the schematic diagram of the MIR system in TPE-RX [12]. It consists of an optical system and a 2D receiver system. The quartz window of the TPE-RX viewing port is located at $r = 67$ cm. The RF wave illuminating from the horn antenna is reflected by the first plain mirror (M_1). The RF wave passes through the first beam splitter (BS_1) to the main mirror (M_2). The main mirror, which is an elliptic concave mirror with the size of 40 cm in diameter at $r = 140$ cm, makes a parallel illumination beam in the plasma. The reflected wave is collected by the main mirror and is separated from the illumination beam by the first beam splitter (BS_1). The local oscillation (LO) wave and the reflected wave are mixed at the second beam splitter (BS_2). The image of the plasma fluctuation is made on the detector surface by the Teflon lens (L_1). The optical system has been designed and tested carefully, and good agreement between the measured beam profiles and those obtained by a ray tracing simulation was confirmed.

The receiver system consists of a planer Yagi-Uda antenna, a Schottky barrier diode, low pass filter, intermediate frequency (IF) amplifier and phase-detector. The Yagi-Uda antenna array is made on the Teflon printed circuit board (PCB). On the design of antenna system, a computer code for electro-magnetic field is employed. The 4 by 4 2D antenna and detector circuits are made by the micro strip line technology, which enables high sensitivity measurement. 4 elements are set on a PCB with a distance of 12 mm, and 4 PCBs are stacked with a distance of 15 mm.

The spatial resolution of the detector array in the plasma is about 3.7 cm.

A Gunn oscillator generating the microwave with frequency of 20 GHz is used. The RF wave illuminates in the O-mode, so the cutoff density is $n_{\text{cut}} = 0.5 \times 10^{19} \text{ m}^{-3}$. The LO wave with the frequency of 20.11 GHz is made by mixing the RF wave (20 GHz) and the low frequency wave (110 MHz) at an up-converter. By mixing the reflected wave and the LO wave, the 2D mixer array makes IF signal of 110 MHz. This IF signal contains the amplitude A and the phase ϕ of the density fluctuation in plasma. The amplitude is obtained by rectifying the IF signal with a diode detector. The phase is obtained by comparing the IF signal and the mixed signal by the phase demodulator.

3. Analysis Technique

3.1 2D cross-correlation

The two-point cross-correlation [13] is a standard analysis method to study the correlation between two fluctuations, given as

$$\Gamma_{ij} = \langle n_i n_j \rangle = \int_{\Delta t} \int_{\Delta \omega} n_i(\omega, t) n_j^*(\omega, t) d\omega dt \quad (1)$$

where the asterisk $*$ denotes complex conjugation, $n(\omega, t)$ is the Fourier transform of the time series, i and j represent different channels. The cross-correlation spectrum array can be obtained by doing the cross-correlation between the reference channel and every channel in the detecting region. The cross-correlation spectrum is the inverse Fourier transforms of the power spectrum. According to the Wiener-Khinchin theorem, the power spectrum is the Fourier transform of the autocorrelation function, defined as

$$S(k_x, k_y) = \iint \Gamma(x, y) e^{-i(k_x x + k_y y)} dx dy \quad (2)$$

where, k_x and k_y are the toroidal and the poloidal wavenumbers, respectively. $\Gamma(x, y)$ is the average autocorrelation array which is averaged over different reference channels. Figure 2 shows the 2D power spectrum estimated by equation 2. The spectrum is dominated by a broad peak with sidelobes. It may conceal the other modes which have small power density. Therefore, the standard Fourier transform fails to resolve the spectral peaks.

3.2 MEM

The power spectrum estimated by Fourier transform is similar as using a bandpass filter in the unknown autocorrelation function we want to solve. If one can extend the correlation measurements outside the measured region, the power spectrum with high resolution can be restored. One possible way is trying to find the filter coefficients by autoregressive method. However, the result is sensitive to the noise and is not very reliable sometimes. It may cause spurious peaks if we fail to set the convergence condition

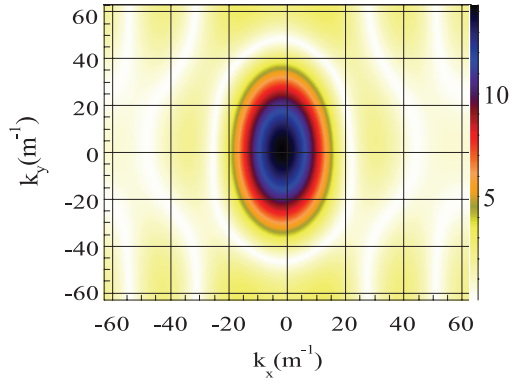


Fig. 2 The power spectrum $S(k_x, k_y)$ obtained by Fourier transform. The k_x and k_y are the toroidal and poloidal wavenumbers, respectively.

and fail to select the optimum order of the autoregressive filter. So far, many numerical methods such as autoregressive, maximum likelihood method and Pisarenko methods have been used to the power spectral estimation. Among them, 2D MEM is the most powerful and effective method because of better spectral resolution [9, 10]. In this study, the Skilling MEM will be used, because it is a model-free method which can give more reliable result than the other MEM algorithms, for example the method based on the autoregressive model. The entropy is defined as

$$H(S) = \iint \log(S(k_x, k_y)) dk_x dk_y. \quad (3)$$

The constrained statistic, chi-squared, is used to estimate the misfit between the experimental value and expectation value.

$$C(S) = \chi^2(S) - \chi_{\text{tar}}^2 = \sum_{i=1}^{N_{\text{ch}}} (\Gamma_{\text{meas.}} - \Gamma_{\text{aim}})^2 / \sigma^2 - \chi_{\text{tar}}^2. \quad (4)$$

The entropy is changed to solve the following equation in maximum.

$$P(S) = H(S) - \lambda C(S) \quad (5)$$

under the constraint of $C \rightarrow 0$. Here λ is the Lagrange multiplier. $\Gamma_{\text{meas.}}$ is the 2D autocorrelation function given by equation 1. Γ_{aim} is the autocorrelation function estimated by MEM. σ is the standard error of $\Gamma_{\text{meas.}}$. χ_{tar} is the target to converge maximum of equation 5 within reasonable calculation time. The maximum condition is satisfied when $\Gamma_{\text{meas.}} = \Gamma_{\text{aim}}$ and it is possible for the 1D MEM. However, the maximization process of equation 5 in 2D array requires non-linear optimization. χ_{tar} should be equal to channel number but it is determined empirically for good convergence. This problem is solved iteratively by searching for maximum entropy over three well chosen search directions [10, 14].

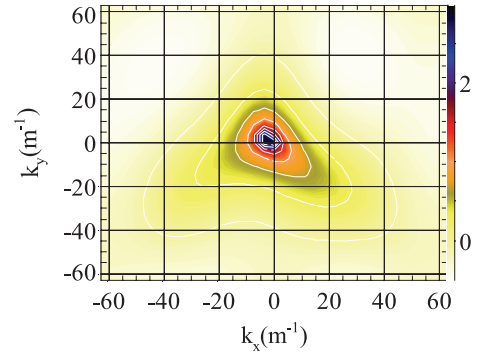


Fig. 3 The power spectrum $\log(S(k_x, k_y))$ of PPCD plasma obtained by MEM. The k_x and k_y are the toroidal and poloidal wavenumbers, respectively.

Figure 3 shows the power spectrum $\log S(k_x, k_y)$ estimated by using MEM in PPCD plasma. Note that the logarithm axis is used. The peak in the power spectrum is much higher than the background fluctuations. Therefore, the k -spectrum estimated by MEM has high 2D spectral resolution.

4. Turbulence of PPCD and High Θ Plasmas

The RFP configuration is generated by the relaxation process and sustained by the dynamo effect, which is driven by turbulences and instabilities. The RFP plasma can be also sustained by PPCD. The nonlinear MHD dynamo model is used to explain the dynamo mechanism [15]. This model assumes that the fluctuation induced electromotive force sustains the field aligned current against resistive decay. The parallel mean-field Ohm's law can be written as

$$\eta j_{\parallel} = E_{\parallel} + \langle \tilde{v} \times \tilde{B} \rangle_{\parallel} \quad (6)$$

where, η is the electric resistivity. j_{\parallel} is the parallel equilibrium current, \tilde{v} , \tilde{B} are the fluctuating fluid velocity and magnetic field, respectively. $\langle \rangle$ denotes the average over an equilibrium flux surface. $\langle \tilde{v} \times \tilde{B} \rangle_{\parallel}$ represents the dynamo term. E_{\parallel} is the external electric field generated by PPCD. In PPCD operation, E_{\parallel} drives the poloidal current, so that the Taylor state is sustained without the help of the dynamo. As a result, the dynamo related fluctuations can be suppressed. In high Θ plasma the dynamo is dominant. Here, the pinch parameter Θ is defined as the ratio of the poloidal magnetic field at the edge to the volume averaged toroidal magnetic field, $\Theta = B_p(a) / \langle B_t \rangle$. The high Θ is defined as $\Theta > 1.6$. The fluctuation becomes more coherent and the fluctuation amplitude of the magnetic probe is increased as the Θ is increased. The sawtooth crashes are often observed during high Θ operation [16].

The turbulences of PPCD and high Θ plasmas are compared between the 2D k spectra estimated by MEM. As shown in Fig. 3, the spectral peak is observed at $k_x =$

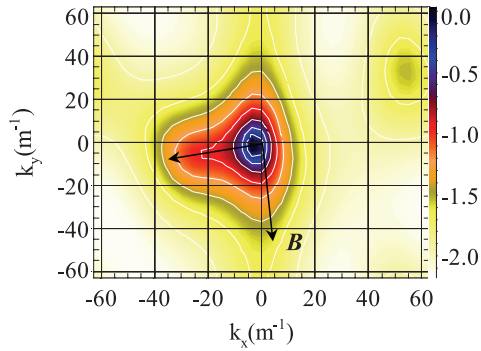


Fig. 4 The power spectrum $\log(S(k_x, k_y))$ of high θ plasma estimated by MEM. The k_x and k_y are the toroidal and poloidal wavenumbers, respectively.

$-3 \pm 3 \text{ m}^{-1}$ and $k_y = 3 \pm 3 \text{ m}^{-1}$ in PPCD plasma. The mode energy is limited at the low k range which suggests low turbulence in PPCD plasma. The dominant mode is $m = 1/n = -7$ with the error of $\Delta m = 1/\Delta n = 7$. This is the single helicity mode which is often observed in PPCD plasma in TPE-RX. Figure 4 shows the power spectrum $\log(S(k_x, k_y))$ of high θ plasma. The spectral peak is observed at $k_x = -3 \pm 5 \text{ m}^{-1}$ and $k_y = -3 \pm 6 \text{ m}^{-1}$. The dominant modes are $m = -1 \pm 2/n = -7 \pm 14$. It is wider than that of PPCD plasma. Therefore, the spectrum of high θ plasma expands to the high k range.

The reversed surface can be obtained by the modified Bessel function model [8]. Generally, the reversed surface is about $r/a = 0.9$ in the high θ plasma, while it is about $r/a = 0.8$ in the typical PPCD plasma due to the driving of the external field. In PPCD plasma, the cutoff surface is about $r/a = 0.85$ due to the high electron density. MIR detects the density fluctuation outside of the reversed field surface. In the high θ plasma, the cutoff surface is about $r/a = 0.75$ due to the low electron density. MIR detects the density fluctuation inside of the reversed field surface.

The evolutions of the tearing modes during a dynamo event have been discussed by using magnetic probe [11, 16]. Those observations show that the multi-modes will be excited during the dynamo event in the high θ plasma. As shown in Fig. 4, the wide k distribution denotes the presence of multi-modes in the high θ plasma.

The expansion direction in k spectrum of the high θ plasma is mainly in toroidal direction which indicates by an arrow shown in Fig. 4. The magnetic field is mainly poloidal near the reversed field surface. The expansion direction is perpendicular to the magnetic field line. It is in the electron drift direction. Therefore, the turbulence in the high θ plasma propagates in the electron drift direction. The expansion in high k range suggests the strong turbulence in the high θ plasma. This result agrees with the nonlinear MHD dynamo model.

5. Summary and Discussion

In summary, 2D turbulences have been measured by using MIR in TPE-RX. The turbulences between PPCD and high θ plasmas have been studied by using MEM, which provides high spectral resolution. The low k mode is dominant in PPCD plasma, while in high θ plasma the spectrum is broad which suggests presence of multi-modes in the plasma. The k spectrum of the high θ plasma expands to the high k range and the turbulence propagates in the electron drift direction. The preliminary result suggests that PPCD operation suppresses the turbulence, and high θ plasma has strong turbulence. It agrees with the nonlinear MHD dynamo model.

MEM is a new technique to estimate the power spectrum. It allows us to fit as many peaks to the k spectrum as there are unique values of cross-correlation points. As a result, the location of peak k becomes clear especially when the imaged region is smaller than the wave measured. This technique is very useful and can be used in other imaging diagnostics. Nevertheless, MEM may make artefacts when the noise is very high and the detector size is much smaller than the cross-correlation length. To measure the fine structures of the turbulence, the high sensitive detector array with big size and high spatial resolution should be developed.

The authors would like to thank Professor N. Iwama and H. Tanaka for valuable helps and suggestions. This work is carried out as one of the NINS Imaging Science Project (Grant No. NIFS08KEIN0021). This work is also supported by NIFS (Grant No. NIFS08ULPP525), and SO-KENDAI (Grant No. NIFS08GLPP003). A part of this study was financially supported by the Budget for Nuclear Research of the Ministry of Education, Culture, Sports, Science and Technology of Japan, based on the screening and counseling of the Atomic Energy Commission.

- [1] E. Mazzucato, *Rev. Sci. Instrum.* **69**, 2201 (1998).
- [2] H. Park *et al.*, *Rev. Sci. Instrum.* **74**, 4239 (2003).
- [3] E. Mazzucato *et al.*, *Phys. Plasmas* **9**, 1955 (2002).
- [4] Y. Lin *et al.*, *Plasma Phys. Control. Fusion* **43**, L1 (2001).
- [5] M. Ignatenko *et al.*, *Nucl. Fusion* **46**, S760 (2006).
- [6] T. Estrada *et al.*, *Phys. Plasmas* **8**, 2657 (2001).
- [7] S. Yamaguchi *et al.*, *Rev. Sci. Instrum.* **77**, 10E930 (2006).
- [8] H.A.B. Bodin, *Nucl. Fusion* **30**, 1717 (1990).
- [9] Jae S. Lim *et al.*, *IEEE Trans. Acoust. Speech Signal Proc.* **Aassp-29**, 401 (1981).
- [10] J. Skilling *et al.*, *Mon. Not. R. Astron. Soc.* **211**, 111 (1984).
- [11] Y. Yagi *et al.*, *Nucl. Fusion* **40**, 1933 (2000).
- [12] Y. Nagayama *et al.*, *Plasma Fusion Res.* **3**, 053 (2008).
- [13] Ch.P. Ritz *et al.*, *Rev. Sci. Instrum.* **59**, 2201 (1988).
- [14] C.A. Michael *et al.*, *Plasma Fusion Res.* **2**, S1034 (2007).
- [15] H. Ji *et al.*, *Phys. Rev. Lett.* **73**, 668 (1994).
- [16] Y. Hirano *et al.*, *Nucl. Fusion* **36**, 721 (1996).